Comparison of ALICE-II Code Predictions with SRI Complex Vessel Experiments

J.L. Ku
Department of Bioengineering, University of Michigan, Ann Arbor, Michigan 48104, U.S.A.
C.Y. Wang, W.R. Zeuch
Reactor Analysis and Safety Division, Argonne National Laboratory, 9700 South Cass Avenue, Argonne, Illinois 60439, U.S.A.

Several complex vessel experiments on 1/20- scale models of the Clinch River Breeder Reactor Project (CRBR) were performed by SRI International to help evaluate the structural integrity when containment is subjected to HCDAs. Among these experiments SM-3 is a simple model which consists of a radial shield, core barrel, upper internal structure (UIS), and a primary vessel. Tests SM-4 and SM-5 are more complex models than SM-3, which have the additions of a thermal liner, a tapered upper vessel flange, a conical core-support ring, a horizontal baffle, and a curved vessel bottom. These two tests used identical models with the exceptions of heavy instrumentation in SM-5 and unannealed (almost rigid) UIS columns in SM-4. All experiments were well instrumented. The data is of high quality and is suitable for the validation of containment codes.

This paper presents comparisons of the ALICE-II code (Arbitrary Lagrangian Implicit-explicit Continuous Fluid Eulerian containment code - second version) with experiments SM-3 through SM-5. Two calculations are performed with ALICE-II on each of these three experiments, using both the pressure-time histories (p-t) and the pressure-volume relationships (p-v) as input to describe the energy source.

Correlations of the computed pressures with the experimental results at all gauges are made. Wave characteristics and arrival times are also compared. Results revealed that the ALICE-II code predicts the pressure profiles reasonably well. Exceptionally good results are found for the SM-5 test. The code not only reproduces the general shape of the pressure loadings, but also accurately predicts the magnitudes of the pressures.

The calculated strains and vessel deformations for SM-3 to SM-5 tests are also in good agreement with the experimental measurements. In all the calculations, three distensions are evident along the vessel walls. The ALICE-II code closely predicts the location of the distensions and the respective strains. Note that ALICE-II also predicts the upward displacement of the UIS well. For instance, in the SM-3 test the code calculates a displacement of 1.47 cm compared to the experimental result of 1.40 cm. Furthermore, better results are obtained if pressure-time histories (p-t) are used to describe the energy release.

The good agreement obtained demonstrates that the ALICE-II code can predict accurately the complex excursion phenomena and the primary containment response during an HCDA. Using the hybrid Lagrangian-Eulerian mesh to describe the coolant motion, difficulties associated with a pure Lagrangian or Eulerian method have been avoided and the applicability of the code for the reactor safety analysis is greatly extended.

1. Introduction

Safety evaluation of liquid-metal fast breeder reactors (LMFBRs) involving an HCDA requires the use of computer codes to study the response of the reactor containment system and interactions of the structural components with the surrounding fluids. At ANL, the ALICE-II code [1-3], which is based on the state-of-the-art arbitrary Lagrangian-Eulerian method, was developed for that purpose. Its analyses include wave propagation, slug impact, sodium spillage, HCDA bubble migration, coolant cavitation, and flow through perforated upper internal structure (UIS), as well as the containment response. However, before applying the code to the complicated phenomena mentioned above, validation must be performed first by comparing the computed results with experimental data.

This paper describes comparisons of the ALICE-II calculations with complex vessel experiments SM-3 to SM-5 performed by SRI International [4-5]. The SRI complex vessel experiments were performed to help evaluate the structural integrity of the CRBR containment and to provide data for the purpose of verification and/or modification in the development of containment codes. They are performed on reactor vessels with a calibrated energy source. The test models have well-defined material properties and dimensions with precision tolerances. Thus, the test data can be used with confidence for validating fluid-structure interaction codes.

In order to provide a unique and systematic comparison two calculations are performed with ALICE-II on each of these three experiments, using both the pressure-time histories (p-t) and the pressure-volume relationships (p-v) as input to describe the energy source. However, because the analytical and experimental results for these three tests are quite voluminous, detailed comparisons are presented only for the most complex model, SM-5.

2. Experimental Apparatus

A schematic of SM-3, the simplest of the three models tested, is shown in Fig. 1. The vessel wall, made of Ni 200, is 0.302 cm thick. This material was chosen to simulate the stress-strain properties of Type 304 stainless steel at normal reactor operating temperatures. The core barrel, also made from Ni 200, is shielded from direct loading of the detonation products by a radial shield. This is represented by a combination of two soft aluminum cylinders and six segmented steel rings which are positioned inside the core barrel. A charge canister containing a low density explosive is at the center of the core. This simulates the HCDA loads. Above the core is a Mylar diaphragm preventing water, which simulates the liquid sodium coolant, from entering the core region before detonation. Resting on the Mylar diaphragm is 500 gm of lead shot which simulates the mass of the upper pin and assembly structures.

An upper internal structure (UIS), suspended from the reactor cover by 4 support columns, lies 0.254 cm above the core structure. The UIS is made from nickel-plated aluminum. Nineteen holes of total area equal to 33.74 cm^2 penetrate the UIS axially to model the area occupied by control rods. The columns are made from 1.778-cm-O.D., 0.127-cm-thick, Ni 200 tubes which are approximately 20.32 cm long.

SM-4 and SM-5 are more complex models than SM3 although their basic design and materials are the same. The main differences between the complex and simple models are the additions of a thermal liner, a tapered upper vessel flange, a conical core support ring and horizontal baffle, and a curved vessel bottom. SM-4 and SM-5 are identical models with the two excep-

tions of greater instrumentation in SM-5 and unannealed UIS columns in SM-4. Their more complex nature can be seen in the schematic of the SM-5 test shown in Fig. 2.

3. Mathematical Models

The mathematical model of SM-3 is shown in Fig. 3. Since experimental results show very little upward displacement of the cover head, the reactor cover was modeled as rigid. The two gas regions are defined by the empty fluid zones under the cover and adjacent to the radial shield. The top of the core bubble region corresponds to the location of the Mylar diaphragm. The radial shield is modeled by quadrilateral continuum elements. Adjacent to the radial shield is the core barrel modeled by 10 thin shell elements of thickness 0.254 in. The top node is fixed in the radial direction. The UIS has a central opening of radius 3.28 cm and is flagged as a rigid obstacle. The UIS columns run from the reactor cover down to the top of the UIS and are modeled by 3-D pipe elements. They are offset 0.018 cm to simulate its imperfection. The vessel wall is a flexible boundary modeled by 25 thin shell elements with thickness 0.302 cm along the entire length. The two top elements have increased thicknesses of 0.396 and 1.0 cm to account for the tapered section of the SRI model. The bottom is a rigid boundary.

The models for SM-4 and SM-5 have much greater detail. In addition to the internal structures modeled in SM-3, they contain a core support structure, conical support ring, horizontal baffle and curved vessel bottom, all modeled by thin shell elements for two-dimensional analysis. Also, vessel wall and core barrel thicknesses vary along their lengths due to the thermal liner and additional ring around the core barrel. A filmplot of the mathematical model for SM-4 and SM-5 is included in Fig. 4. For these two cases the UIS has a central opening with radius equal to 3.27 cm.

4. Energy Source Input

It is well known that the solution obtained from the numerical analysis depends strongly upon the input source pressure used in the computer code. Two types of input pressure data can be used in the analysis to describe the behavior of the core-gas bubble; i.e., a pressure time (P-t) history and a pressure volume (P-V) relationship. The pressure time (P-t) history of the core-gas bubble can be obtained relatively easily after the test if pressure transducers were mounted on the core barrel. However, the pressure-time history depends significantly on the reactor configuration. In other words, the pressure-time (P-t) history describing the behavior of the core gas in one reactor cannot apply to the other reactors if they have different configurations.

The pressure volume (P-V) relationship is computed rather complexly from the gauge measurements of the core pressure as well as the corresponding volume increase of the core gas bubble. In the energy-calibration experiments performed by SRI, the core volume increase was computed from the displacement of the upper boundary (free surface) of the water slug together with the water compressibility due to the passage of the compression waves. The displacement of the water slug was measured by means of a light ladder mounted on the water surface, whereas the water compressibility was calculated analytically from acoustic theory based on one-dimensional spherical wave propagation. Because error could be introduced in the determination of the P-V relationship, the source pressure based on the P-V relationship is expected to be less accurate than that of the pressure-time (P-t) history.

5. Results

5.1 Computed Reactor Configurations

To illustrate the ALICE-II calculations, Fig. 5 shows the reactor configuration for experiment SM-5 at t = 3.45 ms after the start of computation. It illustrates: (1) the upward displacement of the UIS and its interaction with the core-gas bubble and the surrounding fluid, (2) the expansion of the core-gas bubble and its distortion as it encounters the sharp corners of various internals, (3) the deformations of the radial shield, core barrel, and the primary vessel which can be visualized from the movements of the fluid grid lines relative to their initial configurations, (4) the fluid movement on both sides of the baffle plate and the core-support skirt, and (5) the deformation of the UIS columns in response to the upward force generated from the reactor core.

5.2 Pressure Loadings

In order to gain some insight into the wave propagation in the compressible fluid due to the presence of various complex internals, the pressure loadings are presented for the most complicated test, SM-5. Figures 6-10 are the most representative pressure-time histories at gauge positions P5, P7, P8, P9, and P10, respectively, using the average core pressure of gauges P1 and P2 as the input source. In these figures the solid lines are the ALICE-II results and the dotted lines are the experimental data.

In general, the calculated pressure loadings agree well with those observed in the experiment. The code not only reproduces the general shape of the pressure loadings but also accurately predicts the magnitudes of the pressures. However, deviations such as an earlier decay of the incident pulse at gauge P7, are observed. Also, the pressure spike generated by slug impact at P10 in Fig. 10 is proceeded by many small spikes. These discrepancies may be attributed to the hydrodynamic treatment and numerical modeling of the perforated UIS. In the ALICE-II calculations, flow through the UIS coolant passageways is assumed to be non-turbulent. Actually, this flow may be very turbulent from converging and diverging flow through the nineteen penetration holes in the UIS. Also, modeling of UIS openings as one central opening rather than nineteen uniformly dispersed holes could cause uneven free-surface motion and introduce error into the analysis.

5.3 Dynamic Strains

The dynamic strain measurement is perhaps the least accurate record in the experimental data compared to other data such as pressure and post-test vessel deformation. A typical strain gauge has difficulty recording strain exceeding 2%. Therefore, the dynamic strain records obtained by strain gauges are not suited for the code-validation purpose, especially for large strain cases. Figure 11 compares the calculated and measured strain histories at gauge SG8, of the SM-5 test, located at the upper vessel wall (see Fig. 2 for its location). Each curve consists of two portions (before and after t = 3 msec) generated by the incident pressure and slug impact pressure, respectively. It can be seen that the predicted shape and magnitude agree well with the experimental findings. Due to the space limitation, comparisons of strains at other gauge locations are not presented here.

5.4 Wall Deformations

The final deformable shapes of reactor vessels and core barrels for tests SM-3 through SM-5 are given in Figs. 12-14, where the calculated results are shown in solid lines and the experimental measurements in dotted lines. Except for test SM-4, experimental measurements were taken at several different meridians as indicated by the spread of the experimental

data. It can be seen that in each test the vessel wall has three distensions. ALICE-II predicts the location very accurately, and overall agreement between the calculated and measured result, is quite good. However, for the SM-3 test, the ALICE-II code slightly overpredicts the core barrel strain and underestimates the deformation of the vessel wall at the UIS region. This may be attributed to the fact that more energy may have been transmitted to the radial shield and core barrel, instead of in the upward direction and around the UIS. Nevertheless, ALICE-II predicts the more complex cases, such as tests SM-4 and SM-5, quite well.

5.5 Comparison of P-V and P-t Results

Separate calculations were performed on tests SM-3 to SM-5 using the P-V relationship provided by SRI as the core pressure input. As mentioned before, the P-V data, derived from the energy calibration experiment, is quite general and applicable to different reactor configurations. However, it is less accurate compared to the P-t input, particularly at the later stage of the excursion when the core-gas bubble starts to contract under the action of the reflected wave generated by the slug impact.

In general the pressure loadings, dynamic strains, and vessel deformations obtained from the P-V input compared reasonably with the P-t results. To illustrate the P-V calculations, Fig. 15 provides comparisons of vessel and core-barrel profiles obtained from analyses with different source terms. It can be seen that both results are quite close, except that the upper vessel deformation generated by the P-V input is overpredicted.

6. Conclusions

It has been demonstrated that the hybrid Lagrangian Eulerian code ALICE-II can be used for calculating the response of the primary containment consisting of complex internals such as the upper internal structure, core-support structure, internal thin baffles, thermal liner, etc. Not only do the computed results accurately describe the propagation of incident pressure waves and subsequent reflections from the nearby boundaries, but they also give slightly conservative results. The ALICE-II code is also extremely efficient; the CPU time for simulating the SM-5 experiment is only 42 min. on an IBM 370/195.

The good agreement between the analytical predictions and the SRI complex vessel experiments lends credibility to the mathematical formulations and numerical techniques used in the ALICE-II code.

7. Acknowledgments

The authors would like to thank Drs. Y. W. Chang and S. H. Fistedis for their encouragement. This work was performed in the Engineering Mechanics Program of the Reactor Analysis and Safety Division at Argonne National Laboratory under the auspices of the U.S. Department of Energy.

References

[1] WANG, C. Y., ZEUCH, W. R., "ALICE-II: An Arbitrary Lagrangian-Eulerian Code for Containment Analysis with Complex Internals," Trans. Am. Nucl. Soc., Vol. 41, p. 364 (June, 1982).

[2] WANG, C. Y., ZEUCH, W. R., "A Multi-Dimensional Arbitrary Lagrangian Eulerian Method for Dynamic Fluid-Structure Interaction," Fluid-Transients and Fluid/Structure Interaction, eds., Y. W. Shin, F. J. Moody, M. F. Au-Yang, 1982 ASME Special Publication PVP-64, Book No. H00221, pp. 289-316 (June, 1982).

[3] WANG, C. Y., ZEUCH, W. R., "Recent Developments of the Arbitrary Lagrangian-Eulerian Containment Code ALICE-II," Proc. of the 7th Intl. Conf. on Structural Mechanics in Reactor Technology, paper E 4/8, Chicago, IL (August, 1983).

[4] ROMANDER, C. M., CAGLIOSTRO, D. J., "Structural Response of 1/20-Scale Models of the Clinch River Breeder Reactor to a Simulated Hypothetical Core Disruptive Accident," SRI Project PYU 3929, Technical Report 4 (October, 1978).

[5] ROMANDER, C. M., CAGLIOSTRO, D. J., "Structural Response of a 1/20-Scale Model of the CRBR to a Simulated HCDA," Proc. of the 5th Intl. Conf. on Structural Mechanics in Reactor Technology, paper E 5/4, Berlin, Germany, August 13-17, 1979.

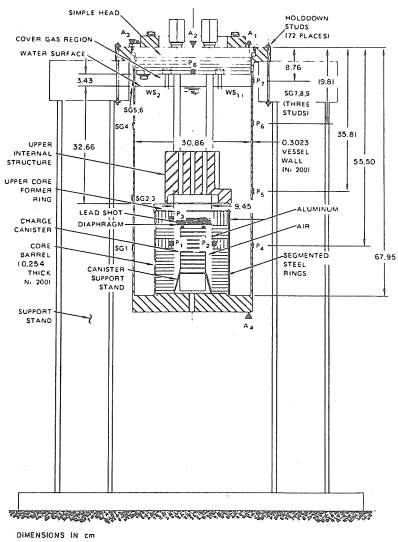

1. SM-3 with Instrumentation

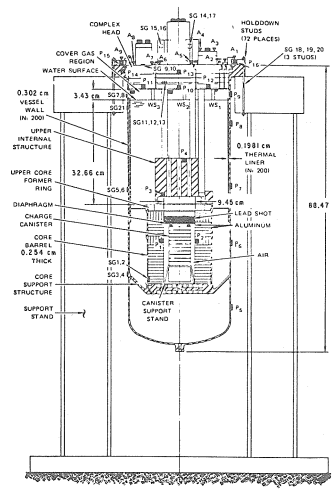

2. SM-5 with Instrumentation

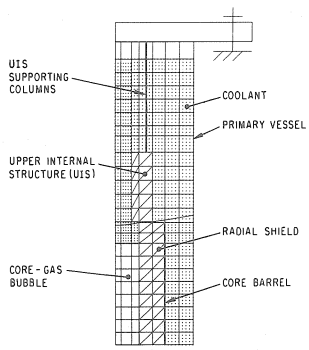

3. Mathematical Model of SM-3

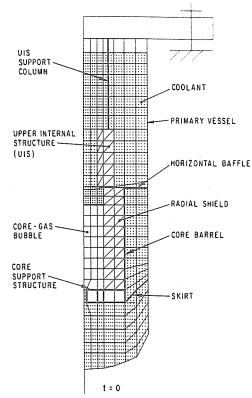

4. Mathematical Model of SM-4 and SM-5

J.L. Ku
*Present address: Department of Bioengineering, The University of Michigan, Ann Arbor, MI 48104, U.S.A.

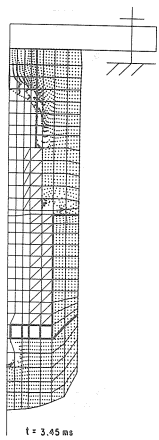

5. SM-5 Configuration at 3.45 ms

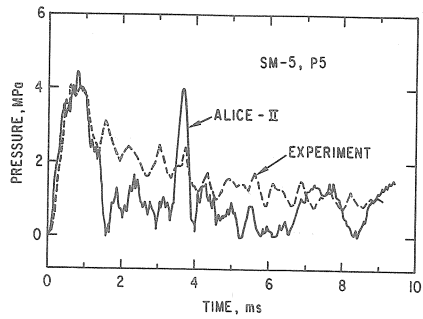

6. Comparison of Pressure Loadings at Gauge P5 (Lower Vessel)

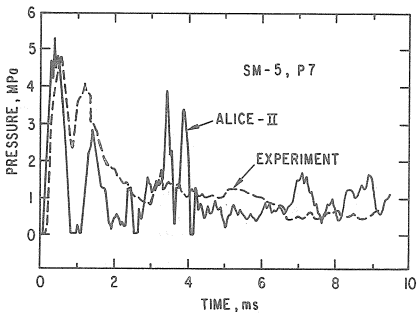

7. Comparison of Pressure Loadings at Gauge P7 (Vessel Wall at UIS)

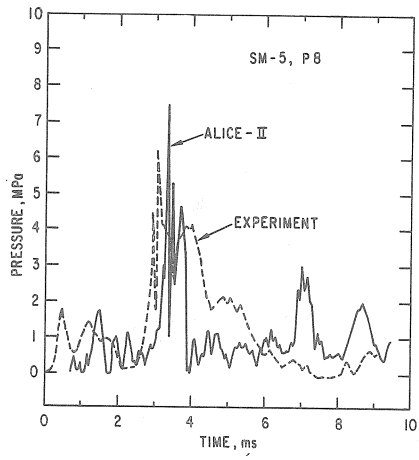

8. Comparison of Pressure Loadings at Gauge P8 (Vessel Wall)

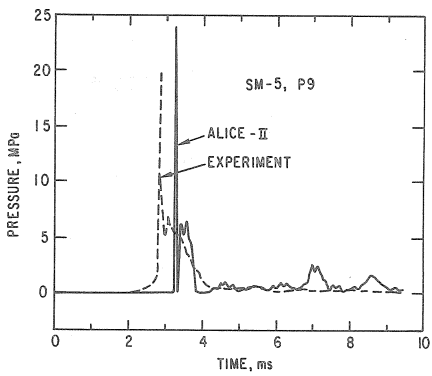

9. Comparison of Pressure Loadings at Gauge P9 (Upper Vessel Wall)

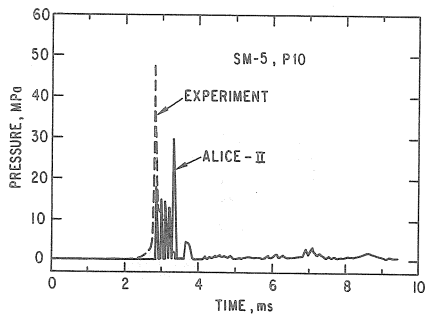

10. Comparison of Pressure Loadings at Gauge P10 (Center of the Head)

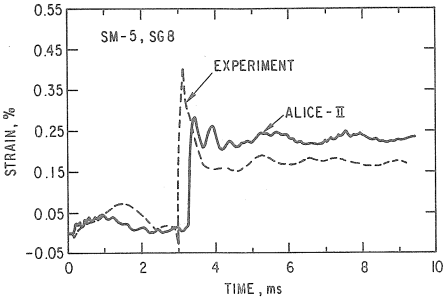

11. Comparison of Strain Histories at Gauge SG8 (Upper Vessel Wall)

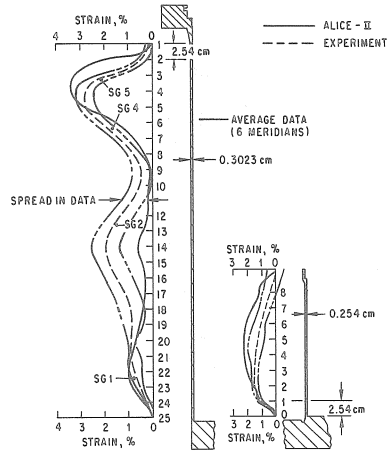

12. Deformed Shape Profiles of SM-3

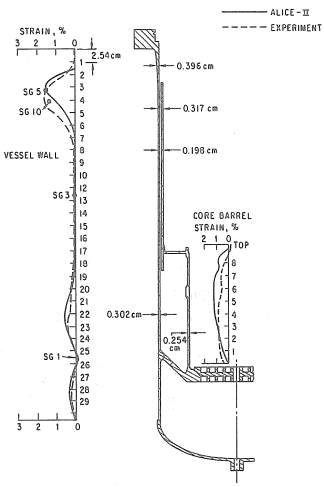

13. Deformed Shape Profiles of SM-4

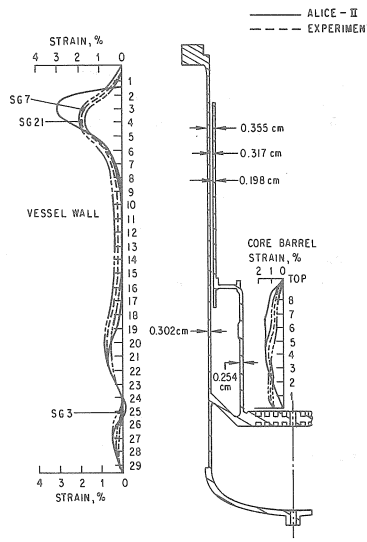

14. Deformed Shape Profiles of SM-5

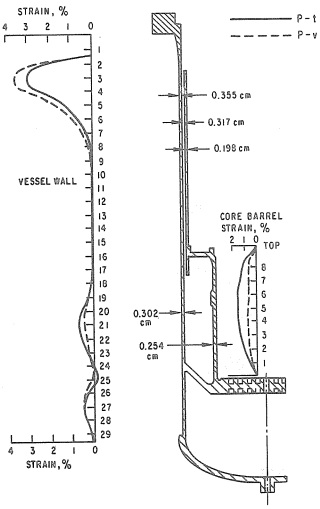

15. Deformed Shape Profiles of SM-5 (P-t vs P-V)